

# Rod-like cyanophenyl probe molecules nanoconfined to oxide particles: Density of adsorbed surface species

Stefan Frunza<sup>1</sup>, Ligia Frunza<sup>1,a</sup>, Constantin Paul Ganea<sup>1</sup>, Irina Zgura<sup>1</sup>, Ana Rita Brás<sup>2</sup>, and Andreas Schönhals<sup>3</sup>

<sup>1</sup> National Institute of Materials Physics, R-077125 Magurele, Romania

<sup>2</sup> Department Chemie, Institut für Physikalische Chemie, Universität zu Köln, D-50939 Köln, Germany

<sup>3</sup> Bundesanstalt für Materialforschung und prüfung (BAM), D-12205 Berlin, Germany

Received: 10 November 2015

Published online: 2 February 2016 – © Società Italiana di Fisica / Springer-Verlag 2016

**Abstract.** Surface layers have already been observed by broadband dielectric spectroscopy for composite systems formed by adsorption of rod-like cyanophenyl derivatives as probe molecules on the surface of oxide particles. In this work, features of the surface layer are reported; samples with different amounts of the probe molecules adsorbed onto oxide (nano) particles were prepared in order to study their interactions with the surface. Thermogravimetric analysis (TGA) was applied to analyze the amount of loaded probe molecules. The density of the surface species  $n_s$  was introduced and its values were estimated from quantitative Fourier transform infrared spectroscopy (FTIR) coupled with TGA. This parameter allows discriminating the composites into several groups assuming a similar interaction of the probe molecules with the hosts of a given group. An influence factor  $H$  is further proposed as the ratio of the number of molecules in the surface layer showing a glassy dynamics and the number of molecules adsorbed tightly on the surface of the support: It was found for aerosil composites and used for calculating the maximum filling degree of partially filled silica MCM-41 composites showing only one dielectric process characteristic for glass-forming liquids and a bulk behavior for higher filling degrees.

## 1 Introduction

Studies of molecules confined to nano/micropores have both fundamental and practical interests (for instance [1–3] or a recent review [4]). The fundamental interest is related to the relevance of a length scale responsible for glassy dynamics, phase transitions, or in general finite-size effects. The practical one might lead to technological strategies to manipulate or to stabilize unstable states and/or to obtain new materials with tuned properties. Confinement induces disorder, decreases transition temperatures, and may change the order of the transition. It is also expected that confinement and disorder have a considerable influence not only on the structure but also on the molecular mobility and therefore on the relaxation processes as well, yielding to a change in the bulk-like molecular dynamics. Moreover, structurally well-defined monolayers on solid surfaces will allow modeling a large variety of interfacial phenomena.

Firstly, the surface layers consist in molecules bonded to particular sites of the materials surface (mostly powdered oxides). These layers have properties such as certain molecular mobility with characteristic relaxation times, density, etc. differing from those of the bulk molecules. Secondly, further molecules in a distance from the surface can feel the influence of this first tightly adsorbed molecules leading to a certain thickness of a layer which is influenced by the presence of the surface (whole surface layer). This has been discussed in several studies [5–7]. During recent years, molecules with single functional groups [8] confined to porous host systems have received a particular attention: Thus there were mostly rod-like molecules for instance cyanobiphenyls which can form liquid crystals (see Aliev [9] and others [10–13]), further small organics (*e.g.* refs. [14–19]), polymers [7, 20, 21] or even water [22–25].

Concerning the methods to investigate surface species, several experimental techniques exist, but only a few of them can give quantitative information about molecular orientation of the molecules at the interface. However, each of them has its own shortcomings [26], (operate in high vacuum, require large experimental facilities, usually hardly discriminate against bulk contributions etc.). Among these techniques, there are electron scattering and electron energy loss spectroscopy, neutron and X-ray [27] scattering, (synchrotron) X-ray diffraction [28], Brewster angle microscopy,

<sup>a</sup> e-mail: lfrunza@infim.ro

**Table 1.** Hosts used to obtain composites.

Host	Structure	Chemical composition	$S_{\text{BET}}$ specific surface area [m <sup>2</sup> /g]	Pore diameter $\varnothing$ [nm]	Pore volume $V_p$ [cm <sup>3</sup> /g]	Obs.
MCM-41-28	MCM-41	Si	1238	2.8	1.15	[6]
MCM-41-36	MCM-41	Si	884	3.6	0.79	[6]
MCM-41-41	MCM-41	Si	411	4.1	0.478	[6]
SBA-15-68	SBA-15	Si	593	6.8	1.009	[6]
AlSBA-15-84	SBA-15	Al, Si	602	8.4	0.9	[5]
SiSBA-15-172	SBA-15	Si	576	17.2	1.9	[5]
AlMCM-41-36	MCM-41	Al, Si	896	3.6	0.978	[5]
AlMCM-41-46	MCM-41	Al, Si	651	4.6	0.917	[5]
AlSBA-15-75	SBA-15	Al, Si	596	7.5	1.1	[36]
NMS-F-102	<sup>(a)</sup>	Si	794	10.2	1.6	[37]
SBA-15-116	SBA-15	Si	890	11.6	1.9	This work
AlMCM-41-29	MCM-41	Al, Si	906	2.9	0.76	This work
A <sub>380</sub>	Nanoparticles	Si	380	–	–	This work
$\gamma$ -Al <sub>2</sub> O <sub>3</sub>	Microcrystals	Al	196	9.5	0.55	This work

<sup>(a)</sup> NMS-F is a nanoporous molecular sieve with foam-like structure.

autocorrelation spectroscopy, Infrared, Raman, or ultraviolet-visible spectroscopy and ellipsometry. Other techniques are the second-harmonic and/or sum-frequency generation, near edge X-ray absorption fine structure spectroscopy (NEXAFS) [29], nuclear magnetic resonance, and even computer simulations (see for instance [30]), etc.

Here results are reported concerning cyanophenyl derivatives adsorbed on oxide particles. A significant amount of information concerning the structure and other properties of these derivatives is retrieved. The obtained results were compared with data measured for surface species of compounds without cyano groups but with ester groups. Our previous work was re-considered which was related to the “surface” dynamics of cyanobiphenyl derivatives in composites based on molecular sieves [6,31] or aerosol [33–35], investigated by broadband dielectric spectroscopy. In composites based on cyanophenyl derivatives as probe molecules the broadband dielectric spectroscopy evidenced the existence of a surface layer which have a behavior of glass forming liquids in addition to molecular mobility specific for the bulk liquid crystal. The characteristic frequency of the relaxation process due to the surface layer is lower than that corresponding to the relaxation process of the bulk liquid crystal. When the level of the loading decreases under a certain value (depending on the support type) the slow relaxation process due to the surface layer is only observed.

The density of the adsorbed surface species was introduced here as a characteristic of the confined systems which depends on the chemical nature of the components and on the host structure. Its values were estimated by FTIR coupled with thermogravimetry. The value of the surface density discriminates the composites into several groups. This fact allows assuming a similar interaction of the probe molecules with the surface of hosts belonging to a certain group.

## 2 Experimental

### 2.1 Materials

As probe molecules cyanoderivatives of the 4-cyano-4'*n*-alkylbiphenyl series (from La Roche, Merck, Aldrich) were used as monocomponents where the length of the alkyl tail was widely varied as follows: ethyl (2CB), propyl (3CB), butyl (4CB), pentyl (5CB), hexyl (6CB), heptyl (7CB), and octyl (8CB). The nematic mixture E7 (a mixture of 5CB, 7CB, 4-cyano-4'-oxy-*n*-octylbiphenyl and 4-cyano-4'*n*-pentylterphenyl, from Merck and Qingdao QY Liquid Crystal Co.) was used as well. As an example for an ester compound pentylphenyl pentylbenzoate, (5PEP5) related to the discussed cyanoderivatives was also considered for comparison.

Silica or alumino-silica molecular sieves served as host materials to confine the probe molecules. These sieves were from MCM-41 or SBA 15 type consisting of grains with micrometer size. Each grain contains parallel cylindrical pores arranged in a 2D hexagonal lattice. Hydrophylic aerosil (Degussa Hüls) of type 380, with a surface area of 380 m<sup>2</sup>/g and  $\gamma$ -alumina (ICECHIM, see, *e.g.*, [36]) were used as well. The nominal pore diameter was taken as part of the support name. For instance, a diameter of 2.8 nm of the molecular sieve MCM-41 is indicated as MCM-41-28. Table 1 collects the systems used here for confinement and some of their relevant properties.

The composite samples were obtained by mixing the cleaned oxide powder with the probe molecules either in liquid state or via a solution route. Details of the employed procedures can be found elsewhere [31, 38]. The excess of the probe molecules are removed by vacuum desorption. Table 1 lists samples which have been studied in the given references. Here the corresponding FTIR and TG data are re-considered. Moreover, there are especially prepared samples to check the correctness of the approach (see below). In the following, the sample label keeps the acronym of probe molecule and the confining host defined in table 1. This means that E7/MCM-41-28 stands for E7 molecules confined to MCM-41-28 as host.

## 2.2 Techniques and equipments

The sample characterization was complex and considered the unfilled host and the confined sample as well. Thus, the structure and surface morphology of the hosts were studied by X-ray diffraction and by optical and electron microscopy, while the interactions of the test molecules with the host due to the confinement were investigated by means of FTIR and reflectance UV-vis spectroscopy.

Nitrogen absorption employing Micromeritics ASAP 2000 was performed in order to obtain the texture information. Experimental details can be found elsewhere (*e.g.* [39, 40]). However, it should be noticed that the pore size is underestimated by this method especially for small pore sizes, because there are one or two layers of nitrogen that are adsorbed tightly on the surface of a pore (giving Brunauer-Emmett-Teller surface area  $S_{\text{BET}}$ ) before capillary condensation.

X-ray diffraction measurements allowed phase identification. They were conducted with a D8 Advance (Bruker-AXS) equipment with  $\text{CuK}\alpha$  radiation ( $K\beta$  radiation was eliminated using a nickel filter). Quantitative data were obtained by Rietveld refining.

Fourier transform infrared spectroscopy was applied in the attenuated total reflection (ATR) or transmission mode with a Spectrum BX II (Perkin-Elmer) instrument by collecting 128 scans at a resolution of  $4\text{ cm}^{-1}$ .

The content of probe molecules in the composites was determined by thermogravimetric (TG) measurements as described elsewhere [41]. The weight loss of the composites was measured up to 800 K, where the organic material is burned while the hosts is stable by increasing the temperature up to 973 K or even higher. From the value of the weight loss and the characteristics of the host the loaded amount of organic molecules was estimated [6]. Moreover, a loading degree can be estimated as ratio of the measured mass of the probe molecules to the maximal mass for complete pore filling. For non-porous hosts the loading degree is defined as the ratio of the oxide host mass to the mass of the probe molecules. The TG measurements were performed with Perkin-Elmer Diamond TG-DTA equipment, under dry air atmosphere with a heating rate of  $10\text{ K min}^{-1}$ .

## 3 Method to estimate the density of adsorbed surface species

The amount of probe molecule in 1 g of dried composite [42] (loading degree) was thus determined by thermogravimetry. The first step in the weight loss curve up to ca 400 K is due to the water evaporation. Therefore, in order to determine the amount of the loaded probe only the weight loss taking place in the temperature interval between 400 and 800 K is considered. When the pores are filled completely, this amount has the maximum value of 100%. However, in some rare cases, the found value is higher than 100% (see table 2). This is due to an excess amount of probe molecules which is still existing as bulk material on the host surface or between the grains.

In order to estimate the density of the surface species, the following assumptions are made:

- the filling is uniform in all the pores;
- all pores have the same filling degree;
- the density of the probe molecule is close to 1:  $\rho_{\text{probe}} \sim 1\text{ g/cm}^3$ .

The ratio  $k$  is defined by the mass of adsorbed molecules  $m_{\text{ads}}$ , to the mass of free molecules  $m_f$  (estimated from FTIR measurements see below):

$$m_{\text{ads}}/m_f = k. \quad (1)$$

Furthermore

$$m_{\text{ads}} + m_f = \Theta V_p \rho_{\text{probe}} \quad (2)$$

holds where  $V_p$  is the volume of the pores in 1 g of the host and  $\Theta$  is the filling degree. The mass of the adsorbed molecules can be expressed as

$$m_{\text{ads}} = (k/(k+1))\Theta V_p \rho_{\text{probe}}. \quad (3)$$

The surface density of adsorbed molecules or the density of surface species  $n_s$  is then

$$n_s = (m_{\text{ads}}/M_{\text{probe}})N_A/S, \quad (4)$$

**Table 2.** The density of the adsorbed surface species for the investigated samples.

No. crt.	Sample	$\Theta^*$ [%]	Mass of loaded matter in 1g of host		$k$	$m_s$ on 1g of host		$N_a$ [molecules/100 nm <sup>2</sup> ]	Obs.
			[g]	[g]		[molecules/nm <sup>2</sup> ]	[g]		
7	E7/AlMCM-41-29	103	0.782	1.23	0.43	1.05	105	This work	
8	5-PEP-5/AlMCM-41-29	217	1.650	1.55	1.00	0.70	70	This work	
11	8CB/SiSBA-15-172	15	0.289	4.55	0.23	1.03	103	[5]	
14	8CB/NMS-F-102	62	0.992	1.13	0.53	1.37	137	[36]	
15	E7/SBA-15-68	63	0.635	0.82	0.28	1.07	105	[6]	
16	5-PEP-5/SBA-15-116	25	0.469	1.55	0.28	0.57	57	This work	
17	5CB/SBA-15-116	29	0.55	2.0	0.37	0.95	95	This work	
18	2CB/SBA-15-116	20	0.308	0.50	0.10	1.04	104	This work	
28	5-PEP-5/A <sub>380</sub>	–	0.172	3.23	0.13	0.61	61	This work	
29	2CB/ $\gamma$ -Al <sub>2</sub> O <sub>3</sub>	–	0.377	0.38	0.10	1.58	158	This work	
33	5-PEP-5/ $\gamma$ -Al <sub>2</sub> O <sub>3</sub>	–	0.266	2.78	0.20	2.2	220	This work	

\* Filling degree higher than 100 is met in the case of an excess of probe molecules still existent on the surface.

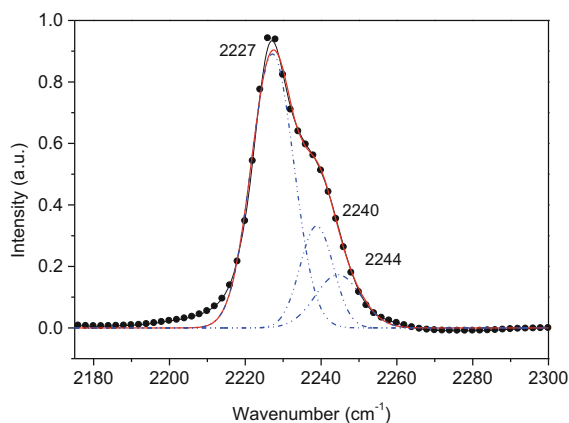


**Fig. 1.** FTIR spectrum in the range of the -CN stretching vibration for the sample 2CB/SBA-15-116 and its decomposition into the different contributions using Gaussians (dot-dashed lines). The numbers correspond to the wavenumbers of the maximum positions.

where  $N_A$  is Avogadro's number,  $M_{probe}$  is the molecular mass of the considered probe molecule and  $S$  is the surface area (in m<sup>2</sup>) of 1 g of the host.  $n_a$  can be estimated using eq. (4) because all the other parameters are known or can be determined from experiments.

## 4 Results and discussion

To estimate the ratio of the mass of adsorbed probe and the mass of nonbonded molecules the composite samples are investigated by FTIR. Figure 1 gives a representative IR spectrum of a composite sample in the wavenumber range of the stretching vibrations of the cyano group [43]. The peak is complex and can be decomposed into Gaussians attributed to different species such as (in the order of decreasing wavenumber) dimer [44] and monomer bulk-like species around 2226 cm<sup>-1</sup>, tilted species appearing at ca. 2230 cm<sup>-1</sup> [45,46], species absorbing at higher wavenumbers than 2230 cm<sup>-1</sup>, are those interacting to the hydroxyl groups of the surface of the host by hydrogen bonds, or species coordinately bonded to Al ions absorbing at around 2270 cm<sup>-1</sup> [36]. The deconvolution procedure of the IR absorption peaks allowed to estimate the area under the peaks belonging to the different components.

For a quantitative discussion of the FTIR spectra of confined cyanophenyl molecules one should keep in mind that the molar absorptivities of the bonded and free CN groups which can be different are not available so that a direct comparison of the integrated intensities is not possible. Nevertheless from the fits the areas under the peaks for the

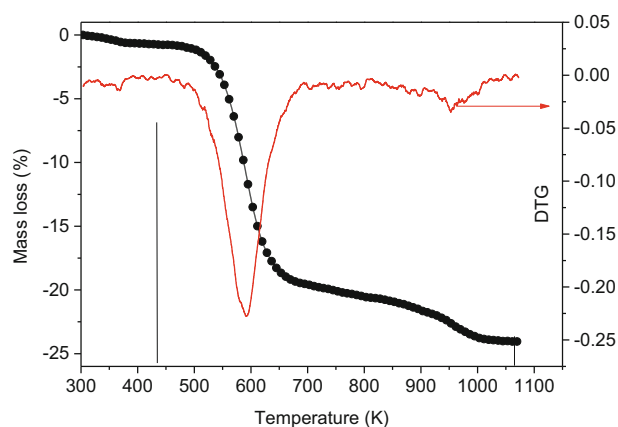


**Fig. 2.** TG curve of the sample 2CB/SBA-15-116 and its derivative. The solid lines indicate the temperature range which is used to estimate the amount of the loaded molecules.

bulk-like contribution  $A_{bulklike}$  and for the strongly interacting probe molecules  $A_{surface}$  are obtained (see also [6]). Since the area is proportional to the number of molecules, the ratio of the two areas would correspond to the ratio of the mass of the species responsible for the absorptions if the absorptivities are assumed to have the same value.

Therefore, the parameter  $k$  mentioned above can be estimated and further the density of surface species can be calculated.

It is found [6] that the interaction parameter  $k$  depends on the pores size. (see also table 1). For the interaction of the molecules with the pore walls, not only the pore size is relevant but also the available surface area. The BET surface area includes the outer surface of the grains and the inner surface inside the pores. Nevertheless, the contribution of the outer surface to the whole specific BET area is less than 8% and can be neglected in the most cases. IR spectroscopy distinguishes between the hydrogen bonded and bulk-like molecules ([43,44] and the literature cited herein).

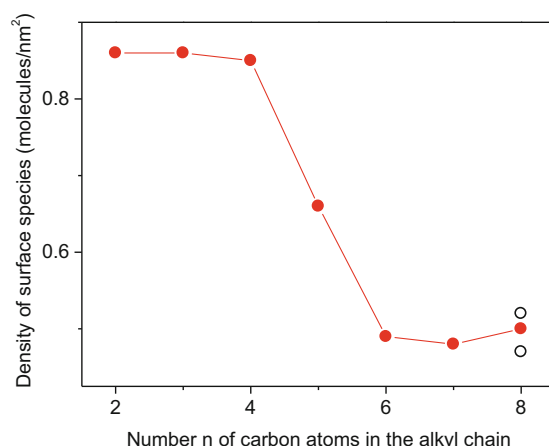
The decomposition process of the peaks in the IR spectra was performed in the case of the composites with 5-PEP-5 too. In that case the stretching vibration of the ester group [47] and especially its carbonyl part [7] is considered as in related cases.

Figure 2 shows the thermogram corresponding to the same sample as depicted in fig. 1. Several processes can be observed which can be ascribed to water desorption, thermal decomposition of different parts of the adsorbed molecule and to desorption processes [41]. The hydration level is less than 1%, confirming that the mesopores are filled with probe molecules, while the water adsorbed onto the external surface is negligible. By this way one can estimate the amount of the probe molecules in the composite. Then the estimation of the surface density of probe molecules bonded to the surface is straightforward according to the eq. (4): The results are presented below in table 2 (the composite samples were mostly arranged according to their hosts) and in figs. 3 and 4. The values for some samples come from the references reported (for the supports in table 1) but the most of the data were obtained in this work.

Figures 3 and 4 illustrate the surface density of molecules adsorbed onto different composites. Thus, in the composites based on aerosil A<sub>380</sub> and probe molecules of the cyanobiphenyl series, the variation of the estimated density of surface species as function of the alkyl chain length is shown in fig. 3. A clear dependence of  $n_a$  on the chain length is observed. For 2CB, 3CB and 4CB a value of  $n_a$  of 0.80 molecules/nm<sup>2</sup> was estimated while for the composite with 6CB, 7CB and 8CB  $n_a$  has a value of 0.50 molecules/nm<sup>2</sup>. 5CB is placed in between in both groups of probe molecules with a  $n_a$  value of 0.66 molecules/nm<sup>2</sup>. This can be understood by considering that the longer alkyl tail will shield possible adsorption sites. The  $n_a$  value of 0.66 molecules/nm<sup>2</sup> is close to that found for the probe molecule 5-PEP-5 (table 2) which is even more bulky than cyanobiphenyls. Figure 4 shows the density of surface species adsorbed onto supports with different aluminum content. The Al ions having complexing properties might bond additional probe molecules than the OH groups on the silica surface [48].

The following conclusions are drawn from the  $n_a$  values given in table 2 and figs. 3 and 4: The composites with a support structure of MCM-41-type with different pore sizes and the probe molecules of E7 have  $n_a$  values of 0.66–0.7 molecules/nm<sup>2</sup>. The alkyl chain of the molecules in E7 has at least 5 methylene groups. Thus, the molecules of this mixture might be compared with those of other probes like 5CB or higher cyanobiphenyl homologous molecules for the composites containing A<sub>380</sub>. The values of  $n_a$  for 5CB/A<sub>380</sub> composites calculated with a specific surface area of 380 m<sup>2</sup>/g of A<sub>380</sub> are in accordance with the  $n_a$  value for E7/MCM-41-36. These results suggest that the bonding of the molecules to aerosil is not influenced by the expected agglomeration of the silica particles. The values of  $n_a$  in the case of Al containing molecular sieves, were found higher than for those containing only Si.

In the composites of SBA-15-68 with E7, the  $n_a$  values are close/a bit greater than 1 molecules/nm<sup>2</sup> although the molecular sieve is built also from silica as in the case of aerosil. In fact, a similar behavior is shown for all molecular



**Fig. 3.** Dependence of the density of surface species as function of the number of carbon atoms in the alkyl chain of cyanobiphenyls in composites based on aerosil A<sub>380</sub>. The lines are guide for eyes. The three values for the sample 8CB/A<sub>380</sub>, correspond to different loading degrees.

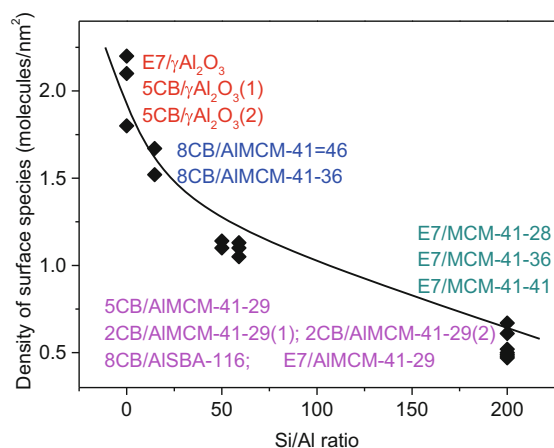


**Fig. 4.** Dependence of the density of surface species as function of the Al content in the samples of indicated type. For simplicity, the samples containing only silica were represented as having Si/Al=200. The line is guide for eyes.

sieves of the SBA-15 type investigated here. This fact gives a hint on the influence of the structural details (pore size, molecular volume) on the adsorption of test molecules on these materials.

At the same time, in the composites where the oxide support contains Al ions,  $n_a$  goes from ca. 1 molecule/nm<sup>2</sup> for AlMCM-41-29 and SBA-15-116, with 5CB to ca. 2.1 molecules/nm<sup>2</sup> for  $\gamma$ -Al<sub>2</sub>O<sub>3</sub> with 5CB or E7.

Composites of 8CB/A<sub>380</sub> with various loadings [36] as studied by dielectric spectroscopy have shown the same value for  $n_a$ . At the same time the mass ratio of aerosil/8CB where the relaxation process characteristic for the bulk disappears is approximately 7 while the whole amount of 8CB which is completely adsorbed for a mass ratio aerosil/8CB of ca. 10 (see fig. 3, in which almost the whole amount of probe molecule is bonded to the host surface for the 3rd 8CB/A<sub>380</sub>).

Taking into consideration the behavior of the surface layer and its dielectric properties, one can define an *influence factor*  $H$  as the ratio of the number of molecules in the surface layers showing a glassy dynamic behavior and the whole number of molecules adsorbed on the surface of the support. This influence factor depends on the interaction of the molecule with the host surface and of the molecules themselves. For the composite aerosil/8CB discussed above having the value 7 for the ratio aerosil/8CB, the factor  $H$  reaches the value 1.47. To find a possible relevancy of such a parameter we used it to estimate the value of the filling degree  $\Theta$  so that bulk relaxation behavior does not begin to manifest itself. One test was performed for a series of MCM-41 molecular sieves (with the diameters of 28, 36, 41, respectively), filled with E7 probe molecule given the similar chemical nature of aerosil and these MCM-41 samples. The estimation took into consideration the specific area of the molecular sieve and the value of  $n_a$  as resulted from the data already reported [5]:

$$\Theta = \frac{HSn_a}{N_A} \frac{M_{probe}}{V_p \rho_{probe}} 100.$$

The value for E7 (as probe molecule) mass and for the filling degree were smaller than those reported; this fact explains the existence of the bulk-like relaxation processes even in these molecular sieves which are partially filled. For a second test the upper filling degree up to which the dielectric relaxation of the bulk is not present was estimated starting from the characteristics of AISBA-15 and SiNMS-F molecular sieves filled with 8CB. The results found for this upper limit of filling factor are 47% and 28.9% (23.7%) respectively and these values are higher than those reported for AISBA-15 (43%) and SiNMS-F (15%) which shows only one dielectric relaxation process characteristic for glass forming liquids.

The volume available for an 8CB molecule as it results from its density is ca.  $0.480 \text{ nm}^3$ . If one takes the length of the molecule as being ca. 2.2 nm into account, one finds a value of ca.  $0.22 \text{ nm}^2$  for the cross section area of the 8CB molecule. If the cyanophenyl molecules were anchored normal to the oxide support surface the surface density should be ca. 4 molecules/ $\text{nm}^2$ . The much smaller values found for the surface density  $n_a$  along with the estimated thickness of the probe molecule layers in the molecular sieves [5] indicate a tilted anchoring of these molecules to the support surface. Such a tilted anchoring was recently found by Velarde and Wang [49], which have shown that the cyano group in a Langmuir monolayer of 4-cyano-4'-*n*-pentylterphenyl is tilted around  $25^\circ \pm 2^\circ$  from the normal of the interface, while that in the 4-*n*-octyl-4'-cyanobiphenyl (8CB) is tilted around  $57^\circ \pm 2^\circ$ , which is consistent with the significant differences in the phase diagrams and in the hydrogen bonding spectra reported in the literature [49]. The need of having 4 neighbors for a bulk-like liquid behavior is already demonstrated [50]. Moreover, the tilting might go up to positioning parallel to the pore walls [51,52].

The samples with 5PEP5 show a density of the surface species similar to those loaded with cyanophenyl derivatives. This fact along with the position of the carbonyl group (responsible for the molecule bonding to the support surface) in the middle of the molecule can be taken as arguments that the molecule lays at small angle on the surface as it was discussed above in the case of cyanophenyl derivatives.

## 5 Conclusions

Properties of the surface layer in composites containing cyanophenyl derivatives as probe molecules and oxide (nano)particles were discussed in connection with their interfacial interactions. Thermogravimetric analysis (TGA) gives the amount of the probe molecules adsorbed on the oxide particles. Data of infrared spectroscopy deliver information on the interaction strength with the oxide surface and the type of bonding to the surface.

Two parameters were proposed: The first one was the density of the adsorbed surface species  $n_s$  which was introduced to characterize the interaction of the probe molecule with the surface. This parameter depends on the nature of the oxide nanoparticles and on the existence of nanopores.

The second parameter is influence factor  $H$  which is proposed as the ratio of the number of molecules in the surface layers with the glassy dynamic behavior and the number of molecules adsorbed on the support surface. The  $H$  value was estimated for 8CB/A<sub>380</sub> composites and it was used for calculating the maximum filling degree of partially filled E7/MCM-41 composites for which the bulk behavior is missing and only the dielectric behavior characteristic for a glass forming liquids is observed.

## Author contribution statement

All authors contributed equally to the paper.

Part of the authors (LF, SF, CPG, and IZ) is indebted to the Romanian Authority for Higher Education, Research, Development and Innovation for financial funding under the Project PN 09450103 belonging to CORE Program. Thanks are given to Prof. V.I. Parvulescu (Bucharest University, Romania) for nitrogen absorption measurements.

## References

1. R. Zorn, B. Frick, H. Büttner H., J. Phys. **IV**, 10 (2000).
2. B. Frick, M. Koza, R. Zorn, Eur. Phys. J. E **12**, 3 (2003).
3. M. Koza, B. Frick, R. Zorn, Eur. Phys. J. ST **141**, 1 (2007).
4. P. Huber, J. Phys.: Condens. Matter **27**, 103102 (2015).
5. L. Frunza, H. Kosslick, S. Frunza, A. Schönhals, Micropor. Mesopor. Mater. **90**, 259 (2006).
6. A.R. Brás, S. Frunza, L. Guerreiro, I.M. Fonseca, A. Corma, L. Frunza, M. Dionísio, A. Schönhals, J. Chem. Phys. **132**, 224508 (2010).
7. M. Füllbrandt, P.J. Purohit, A. Schönhals, Macromolecules **46**, 4626 (2013).

8. C.E.D. Chidsey, D.N. Loiacono, *Langmuir* **6**, 682 (1990).
9. F.M. Aliev, M.N. Breganov, *Sov. Phys. JETP Lett.* **47**, 117 (1988).
10. G.P. Crawford, S. Zumer, *Liquid Crystals in Complex Geometries Formed by Polymer and Porous Networks* (CRC Press, Taylor & Francis Group, London, UK, 1996).
11. A.V. Kityk, M. Wolff, K. Knorr, D. Morineau, R. Lefort, P. Huber, *Phys. Rev. Lett.* **101**, 187801 (2008).
12. X. Zhang, X. Liu, X. Zhang, Y. Tian, Y. Meng, *Liq. Cryst.* **39**, 1305 (2012).
13. S. Calus, L. Borowik, A.V. Kityk, M. Eich, M. Busch, P. Huber, *Phys. Chem. Chem. Phys.* **17**, 22115 (2015).
14. A. Huwe, F. Kremer, J. Kärger, P. Behrens, W. Schwieger, G. Ihlein, Ö. Weiß, F. Schuth, *J. Mol. Liq.* **86**, 173 (2000).
15. A.R. Bras, I.M. Fonseca, M. Dionisio, A. Schönhals, F. Affouard, N.T. Correia, *J. Phys. Chem. C* **118**, 13857 (2014).
16. J. Leys, C. Glorieux, J. Thoen, *J. Non-Cryst. Solids* **353**, 4560 (2007).
17. C.V. Cerclier, M. Ndao, R. Busselez, R. Lefort, E. Grelet, P. Huber, A.V. Kityk, L. Noirez, A. Schönhals, D. Morineau, *J. Phys. Chem. C* **116**, 18990 (2012).
18. B. Frick, C. Alba-Simionesco, G. Dosseh, C. Le Quellec, A.J. Moreno, J. Colmenero, A. Schönhals, R. Zorn, K. Christopoulou, S.H. Anastasiadis, K. Dalnoki-Veress, *J. Non-Cryst. Solids* **351**, 2657 (2005).
19. D. Morineau, C. Alba-Simionesco, *J. Phys. Chem. Lett.* **1**, 1155 (2010).
20. J. Martín, J. Maiz, J. Sacristan, C. Mijangos, *Polymer* **53**, 1149 (2012).
21. M. Krutyeva, A. Wischniewski, M. Monkenbusch, L. Willner, J. Maiz, C. Mijangos, A. Arbe, J. Colmenero, A. Radulescu, O. Holderer, M. Ohl, D. Richter, *Phys. Rev. Lett.* **110**, 108303 (2013) **110**, 119901(E) (2013).
22. P. Kumar, S.V. Buldyrev, F.W. Starr, N. Giovambattista, H.E. Stanley, *Phys. Rev. E* **72**, 051503 (2005).
23. H. Belarbi, A. Haouzi, J.C. Giuntini, S. Devautour-Vinot, M. Kharroubi, F. Henn, *J. Non-Cryst. Solids* **356**, 664 (2010).
24. S. Smirnov, V. Vlasiouk, P. Takmakov, F. Rios, *ACS Nano*. **4**, 5069 (2010).
25. Y. Ryabov, A. Gutina, Y. Feldman, S. Frunza, L. Frunza, A. Schönhals, A. J. Chem. Phys. **133**, 037101 (2010).
26. X. Zhuang, P.B. Miranda, D. Kim, Y.R. Shen, *Phys. Rev. B* **59**, 12632 (1999).
27. G. Cordoyiannis, A. Zidansek, G. Lahajnar, Z. Kutnjak, H. Amenitsch, G. Nounesis, S. Kralj, *Phys. Rev. E* **79**, 051703 (2009).
28. K.H. Liu, Y. Zhang, J.J. Lee, C.C. Chen, Y.Q. Yeh, S.H. Chen, C.Y. Mou, *J. Chem. Phys.* **139**, 064502 (2013).
29. B.H. Clare, K. Efimenko, D.A. Fischer, J. Genzer, N.L. Abbott, *Chem. Mater.* **18**, 2357 (2006).
30. A.K. Soper, *J. Phys.: Condens. Matter* **24**, 064107 (2012).
31. S. Frunza, L. Frunza, A. Schönhals, H.L. Zubowa, H. Kosslick, H.E. Carius, R. Fricke, *Chem. Phys. Lett.* **307**, 167 (1999).
32. S. Frunza, L. Frunza, A. Schönhals, *J. Phys.* **IV**, 10 (2000).
33. S. Frunza, L. Frunza, H. Goering, H. Sturm, A. Schönhals, *Europhys. Lett.* **56**, 801 (2001).
34. S. Frunza, L. Frunza, M. Tintaru, I. Enache, T. Beica, A. Schönhals, *Liq. Cryst.* **31**, 913 (2004).
35. J. Leys, C. Glorieux, J. Thoen, *J. Phys.: Condens. Matter* **20**, 244111 (2008).
36. N.I. Ionescu, M. Chirca, E. Merouiu, J. Herscovici, *React. Kinet. Catal. Lett.* **15**, 425 (1980).
37. L. Frunza, H. Kosslick, U. Bentrup, I. Pitsch, R. Fricke, S. Frunza, A. Schönhals, *J. Molec. Struct.* **651-653**, 341 (2003).
38. G.S. Iannacchione, C.W. Garland, J.T. Mang, T.P. Rieker, *Phys. Rev. E* **58**, 5966 (1998).
39. E. Ilyes, M. Florea, A.M. Madalan, M. Haiduc, V.I. Parvulescu, M.A. Andruh, *Inorg. Chem.* **51**, 7954 (2012).
40. A. Moragues, F. Neațu, V.I. Pârvulescu, M. Dolores Marcos, P. Amorós, V. Michelet, *ACS Catal.* **5**, 5060 (2015).
41. S. Frunza, H. Kosslick, A. Schönhals, L. Frunza, I. Enache, T. Beica, *J. Non-Cryst. Solids* **325**, 103 (2003).
42. A. Hourri, T. Bose, J. Thoen, *Phys. Rev. E* **63**, 051702 (2001).
43. L. Frunza, S. Frunza, M. Poterasu, T. Beica, H. Kosslick, D. Stoianescu, *Spectrochim. Acta Part A* **72**, 248 (2009).
44. G.A. Puchkovskaya, A.Yu. Reznikov, A.A. Yakubov, O.V. Yaroshchuk, A.V. Glushchenko, *J. Mol. Struct.* **381**, 133 (1996).
45. Y.W. Zhou, M. Jaroniec, R.K. Gilpin, *Anal. Chem.* **66**, 4100 (1994).
46. Y.W. Zhou, M. Jaroniec, G.L. Hann, R.K. Gilpin, *Anal. Chem.* **66**, 1454 (1994).
47. S. Frunza, A. Schönhals, L. Frunza, T. Beica, I. Zgura, P. Ganea, D. Stoianescu, *Chem. Phys.* **372**, 51 (2010).
48. A. Bak, K. Chedowska, *Phys. Rev. E* **83**, 061708 (2011).
49. L. Velarde, H.F. Wang, *Chem. Phys. Lett.* **585**, 42 (2013).
50. A. Huwe, F. Kremer, J. Kärger, P. Behrens, W. Schwieger, G. Ihlein, Ö. Weiß, F. Schüth, *J. Mol. Liq.* **86**, 173 (2000).
51. F. Laeri, F. Schüth, U. Simon, M. Wark, *Host-Guest Systems Based on Nanoporous Crystals* (Wiley-VCH, Weinheim, 2003).
52. A.V. Kityk, M. Wolff, K. Knorr, D. Morineau, R. Lefort, P. Huber, *Phys. Rev. Lett.* **101**, 187801 (2008).